RAL-TR-2008-030

Application of the HOTWAXS Detector to Imaging at Higher X-ray Energies (10keV –30keV)

J.E.Bateman[a], D.M.Duxbury[a], I.Harvey[b], W.I.Helsby[b] and E.J.Spill[a]

[a]Science and Technology Facilities Council, Rutherford Appleton Laboratory, Harwell Science and Innovation Campus, Didcot, Oxfordshire, OX11 0QX, U.K.

[b]Science and Technology Facilities Council, Daresbury Laboratory, Keckwick Lane, Daresbury, Warrington, WA4 4AD, UK

8th Oct 2008

Abstract

The HOTWAXS (High Overall Throughput Wide Angle X-ray Scattering) gas detector system, aimed at X-ray diffraction (XRD) and wide angle X-ray scattering (WAXS) applications has been a successful user facility on stations 2.1 and 9.3 at the Daresbury SRS offering high speed data acquisition. The facility has been duplicated on station I22 of the Diamond light source. The energy range covered by stations I22 and 9.3 are very similar varying from 6 to 30keV, well above the energy range conventionally covered by gas detectors. Here we report studies of the options for successful operation of HOTWAXS at the upper end of this energy range, made possible by this particular design.

1. Introduction

The HOTWAXS detector [1] consists of eight pointing anode MSGC [2] modules configured so as to produce a detector of 1024 elements, each with a pointing geometry and a cathode pitch which varies from 409μm at a radius of 400mm to 460μm at a radius of 450mm. For readout purposes the elements are combined in pairs doubling the effective element width. The system utilises a simple channel-by-channel (pixellated) readout method which permits counting at very high rates, with the lower level threshold (LLD) on the discriminator being the only electronic parameter to be set.

Successful phase change studies at beam energies about 8keV are reported elsewhere [3] but the desirability of extending the operation to higher beam energies became apparent. Extension of the use of the detector to the higher energy range raises questions as regards the attendant decrease in the sensitivity and spatial resolution. The loss of stopping power is easily calculated from the x-ray absorption cross-section and is potentially acceptable given the higher beam intensities available from the new SR sources. The degradation of the spatial (i.e. angular) resolution is not simple to estimate. In this report experimental measurements are combined with Monte Carlo modelling to assess the performance of the detector in the higher energy region.

2. X-ray Imaging above 10keV

In the normal operating range (E_x<10keV) the spatial resolution of a gas detector is governed by a convolution of several factors – electronic noise, secondary electron diffusion and the range of the primary photo-electron. As figure 1 shows, this leads to a quasi-normal average footprint on the readout plane [4]. However for E_x>10keV the last factor comes to dominate strongly. Since the projected range of fast electrons in this energy range varies as $\sim E_{pe}^{1.7}$ the degradation in the spatial resolution is a rapid function of E_x. With a conventional centroiding readout method the Full Width at Half Maximum (FWHM) of a pencil beam increases in just this fashion as measured experimentally [5] and by modelling [4]. HOTWAXS uses a radically different (and simpler) readout mode by simply counting events in which the energy deposit in any strip exceeds a simple discriminator level (LLD). As demonstrated by modelling [6] this pixellated approach, while limiting the low energy resolution, leads to a less severe increase in the FWHM as E_x increases, albeit at some sacrifice in sensitivity.

This effect occurs as a result of the particular nature of the X-ray interaction. In argon, a K-shell vacancy (the predominant interaction is on the K shell) is left with a stored energy of 3.2keV dissipated locally in auger electrons with a maximum range of ~200μm. Similarly in xenon an L-shell vacancy energy of 5.1keV is dissipated within about 100μm of the primary interaction. Since these dimensions are small compared to the HOTWAXS strip width (868μm) there is a punctual deposit at the X-ray interaction point of ~115 electrons for argon and 189 electrons for xenon. As the X-ray energy increases the linear deposit of the long-range photo-electron energy in any strip decreases approximately as $E_x/E_x^{1.7}$, so that with a high LLD setting, the extra deposit in the "correct" strip can be preferentially detected. In figure 2 the preservation of a useful

degree of single-channel response is seen in argon at 26keV in spite of the extreme (several mm) width of the average footprint seen in the simulation, figure 1.

The higher density of xenon restricts the photo-electron range and gives a superior FWHM to argon at all higher energies but at greatly increased financial cost (for gas flow conditions) or complexity (for recycled gas). The benefits of a flowing argon/xenon mixture are examined as an affordable compromise. Figure 2 shows the experimental resolution obtained at E_x = 26keV with only 20% of xenon in the argon-DME mixture.

3. Experimental Measurements

A sample of silicon powder has been used as the scattering medium as this exhibits strong diffraction peaks in the angular range between 5 and 65^o. A series of measurements have been performed on station 9.3 of the Daresbury SRS [7] as the beam energy was changed between 10 and 26keV in both an Ar:DME gas mixture (83:17) and an Ar:Xe:DME gas mixture of ratio 63:20:17. A typical diffraction curve obtained from the sample is shown in figure 2 at a beam energy of 26keV for both gas mixtures. The LLD for both cases was set to 0.4 of the beam energy. Figure 3 shows the variation of the spatial resolution as a function of the beam energy for the two gas mixtures (with the LLD at 40% for all beam energies). For the Ar:DME gas mixture, the FWHMs of normal fits to the silicon peaks are much broader than those of the xenon peaks due to the wide tails seen in the peaks (figure 2). However the distributions also have a sharp central spike component. The tails are not seen in the mixture laced with 20% xenon.

A sequence of silicon scattering spectra was acquired with a range of settings of the discriminators (LLD). The peaks of several orders of scattering were measured at each energy and averaged to give smoother data. Figure 4 shows how the FWHM in the argon-DME mixture versus X-ray energy curves systematically improve as the LLD is raised. The cost of this improvement is a corresponding loss of readout sensitivity. Figure 5 shows this behaviour explicitly at E_x = 9.6keV. In this case the counts in a channel of the scattering continuum and the fitted Standard Deviation (σ) of the first order peak are plotted as a function of the LLD (expressed as a fraction of E_x). The drop in sensitivity is quite severe if the LLD is very high ($0.75E_x$) and the spatial resolution asymptotes at one channel ($\sigma=1/\sqrt{12}$) confirming the model ideas described above. Figure 5 also shows that an LLD of $0.4E_x$ is a reasonable compromise between sensitivity and spatial resolution. (The Monte Carlo modelling also indicates that for maximum uniformity of response the LLD should lie close to $0.5E_x$.)

The detection efficiency is a product of the stopping efficiency of Ar (or Ar:Xe) and the readout efficiency. In practical measurements we measure the overall apparent efficiency as we cannot separate out the small fraction of multiple triggers. No absolute measurement of efficiency was possible, but a comparison of the silicon peaks measured under identical experimental conditions, except for the gas filling in the counter, allowed the ratio of the sensitivity to be obtained for the argon-DME and argon-xenon-DME cases. For the two gas mixtures we have used, we observe an increase in count rate of a

factor of ~3 with the addition of 20% xenon over the energy range 10keV to 26keV: see figure 6.

4. Upgrading the system for higher X-ray energies

For routine operation of the system at higher X-ray energies one could envisage two possible upgrade avenues to explore. The first of these is simply the addition of xenon to the gas mixture. As we have seen experimentally, this significantly improves the spatial resolution and the detection efficiency as the X-ray beam energy is increased. Indeed figure 7 shows that at 30keV we would expect an increase in efficiency of a factor of 3 for the addition of 20% xenon, rising to a factor of 10 for pure xenon (both at 30keV). Ideally one would use pure xenon as the stopping gas above 10keV, but we only obtain a good ageing performance with flowing gas. With the current price of xenon one could tolerate running with a fraction of xenon at a reduced gas flow rate but further ageing studies would need to be performed to investigate how the gas flow rate affects the ageing.

The second potential upgrade path would be to instrument each individual anode in the detector, thereby increasing the number of channels to 1024 (and thus reducing the pitch of the readout channels from 868μm to 434μm). The Monte Carlo simulation has been used to check the viability of this option and as the results in figure 8 show, the reduced bin width should improve the spatial resolution substantially giving sub mm FWHM resolution at 30keV, in an Ar:DME gas mixture laced with 20% Xe (because the spread of the residual vacancy signal is still small compared to the bin width). The reduced bin width will produce a worse readout efficiency; see figure 9 which shows that the efficiency drops off by a factor of 2 with half the readout channel width (again at 30keV). Redesign of the preamplifier motherboards and the extra readout electronics would involve significant costs.

5. Discussion

Whilst the HOTWAXS detector has previously been shown to deliver excellent experimental results in its primary energy range (around 8keV), the angular resolution delivered by the system at higher energies in an Ar:DME gas mixture (as with any gas detector) was in question. Monte Carlo modelling of pixellated detector operation predicts that it is possible to maintain useful spatial (angular) resolution at X-ray energies up to 30keV. Here we have shown that by careful setting of the LLD the user has a simple choice of trade off between detection efficiency and position resolution. Indeed with the increased flux of 3rd generation synchrotron sources, the loss of efficiency necessary to obtain good resolution results may be deemed acceptable.

The addition of 20% xenon also radically improves the resolution with the additional benefit of increasing the detection efficiency, albeit with increased running costs due to the xenon. For a flowing gas system such as this, further studies would need

to be performed to assess the viability of running with a reduced flow rate of gas. Indeed the next logical step would be to completely substitute the argon with xenon utilising some form of gas re-circulation and purification system, similar to that used in [8]. The results of figure 3 and 4 should also be investigated further regarding the extended tails seen in the argon peak distributions. With the addition of only 20% xenon these tails disappear which presents a puzzle since the photoelectron range is dependent only on gas density and there is no significant difference between the two mixtures, 1.84g/cm^2 for argon compared to 2.66g/cm^2 for the case with 20% addition of xenon.

The resolution could be further improved by instrumenting each of the 1024 individual channels of the MSGCs as opposed to summing neighbouring anodes, as is the case in the current systems. A dedicated ASIC readout solution (the prototype of which is currently in development) would greatly facilitate this process.

This development has been funded via the facilities development board of the Science and Technology Facilities Council.

References

1. J.E.Bateman, G.E.Derbyshire, G.Diakun, D.M.Duxbury, J.P.A. Fairclough, I.Harvey, W.I.Helsby, J.D.Lipp, A.S.Marsh, J.Salisbury, G.Sankar, E.J.Spill, R.Stephenson and N.J.Terrill, *Nucl. Instr. and Meth. A580 (2007) 1526*
2. A. Oed, Nucl. Instr. & Meth. A261(1988) 351
3. J.E.Bateman, G.E.Derbyshire, G.Diakun, D.M.Duxbury, J.P.A. Fairclough, I.Harvey, W.I.Helsby, S-M. Mai, O.O. Mykhaylyk, G.Sankar, E.J.Spill and R.Stephenson, *IEEE. Trans. Nucl. Sci. 55 (2) (2008) 729*
4. J.E Bateman, Rutherford Appleton Laboratory Report, RAL-TR-2005-010
5. G.C.Smith, J.Fischer, V.Radeka, IEEE Trans. Nucl. Sci. NS-31, No.1, 1984, 111-115
6. J.E Bateman, Rutherford Appleton Laboratory Report, RAL-TR-2006-004
7. G.Derbyshire, B.Dobson, G.N.Greaves, N.Harris, P.Mackle, P.R.Moore, K.J.Roberts, N.Allinson, J.Nicoll, S.Doyle, R.J.Oldman, Rev. Sci. Instrum. 60 (7) (1989) 1897
8. B. Yu, J.A. Harder, J.A. Mead, V. Radeka, N.A. Schaknowski, G.C. Smith *Nucl. Instr. and Meth. A513 (2003) 362*

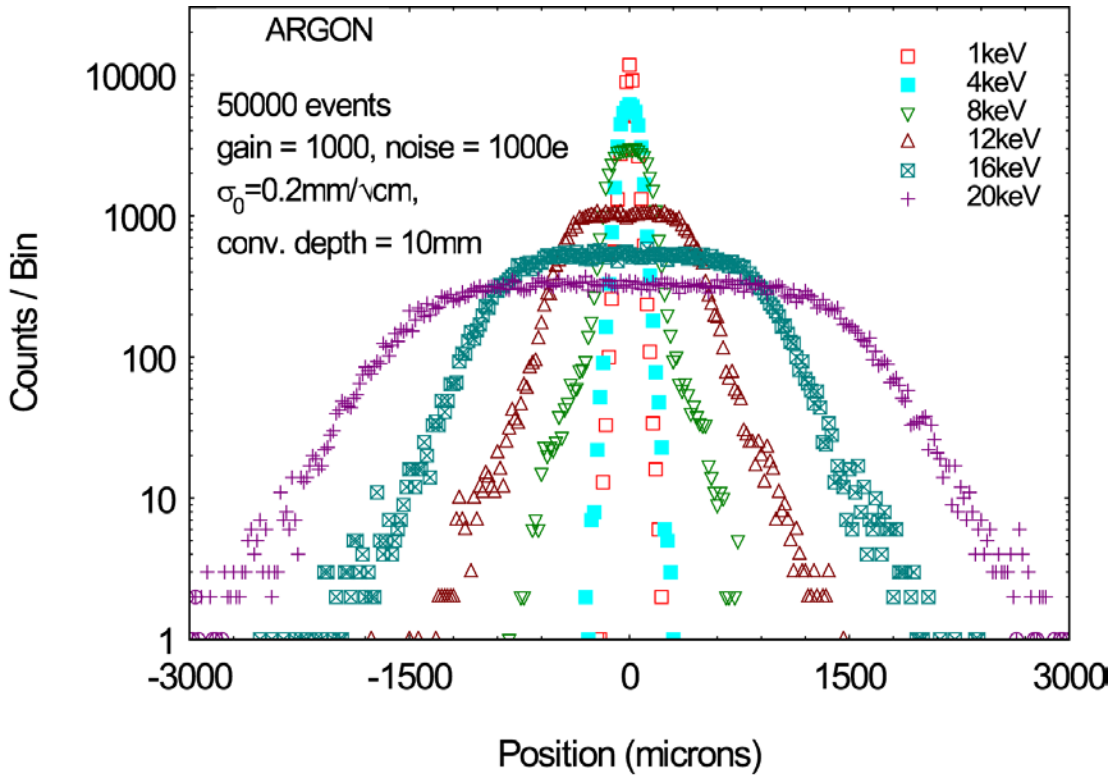

Figure 1: Average charge footprint on the readout plane from [4]

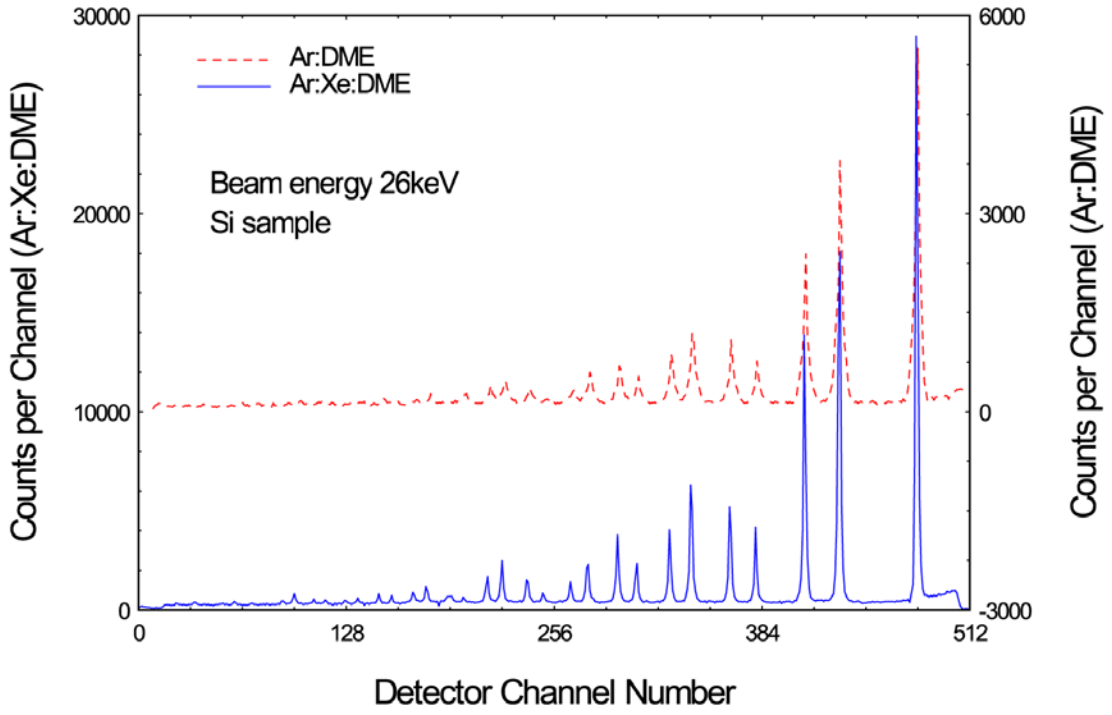

Figure 2: Silicon diffraction data at 26keV in both Ar:DME and Ar:Xe:DME mixtures

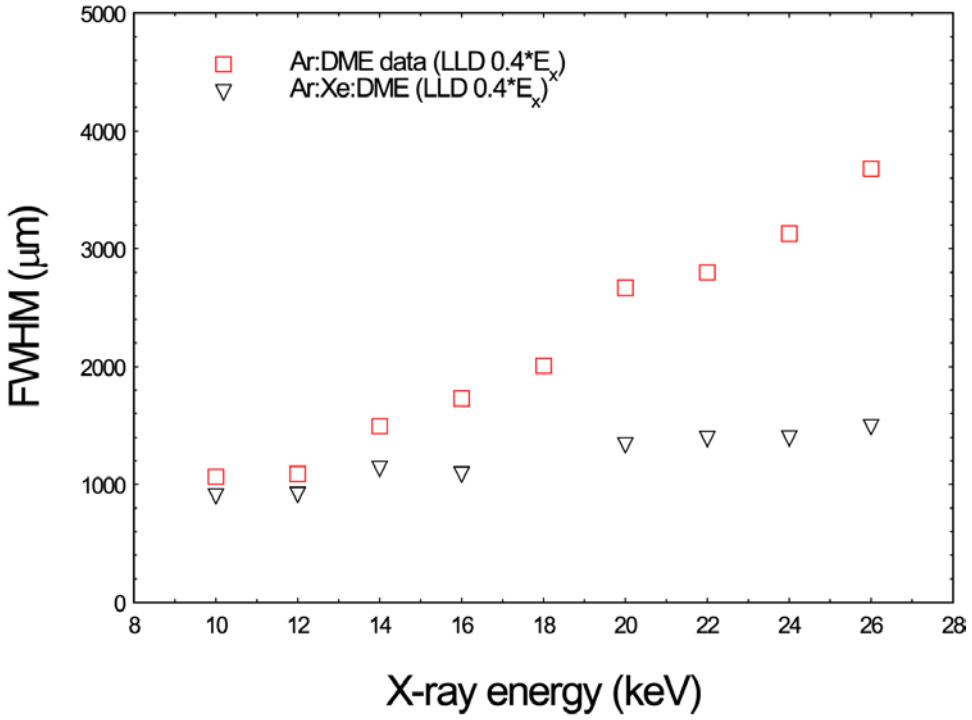

Figure 3: Variation of spatial resolution with beam energy in both Ar:DME and Ar:Xe:DME mixtures

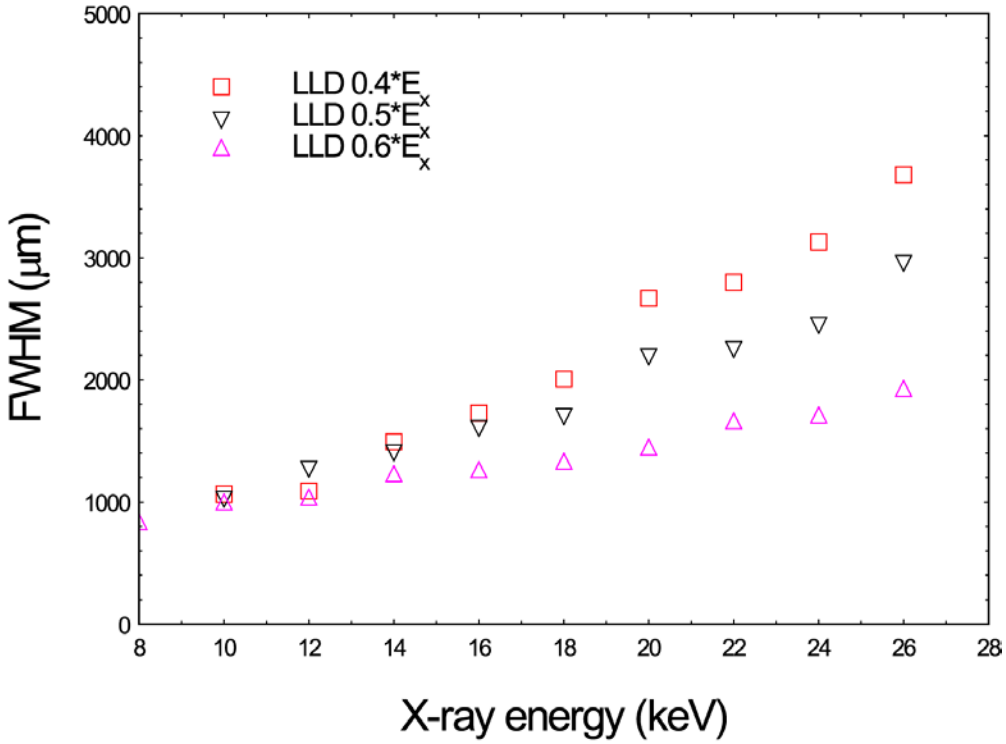

Figure 4: Variation of spatial resolution versus beam energy at various LLD settings in Ar:DME gas mixture

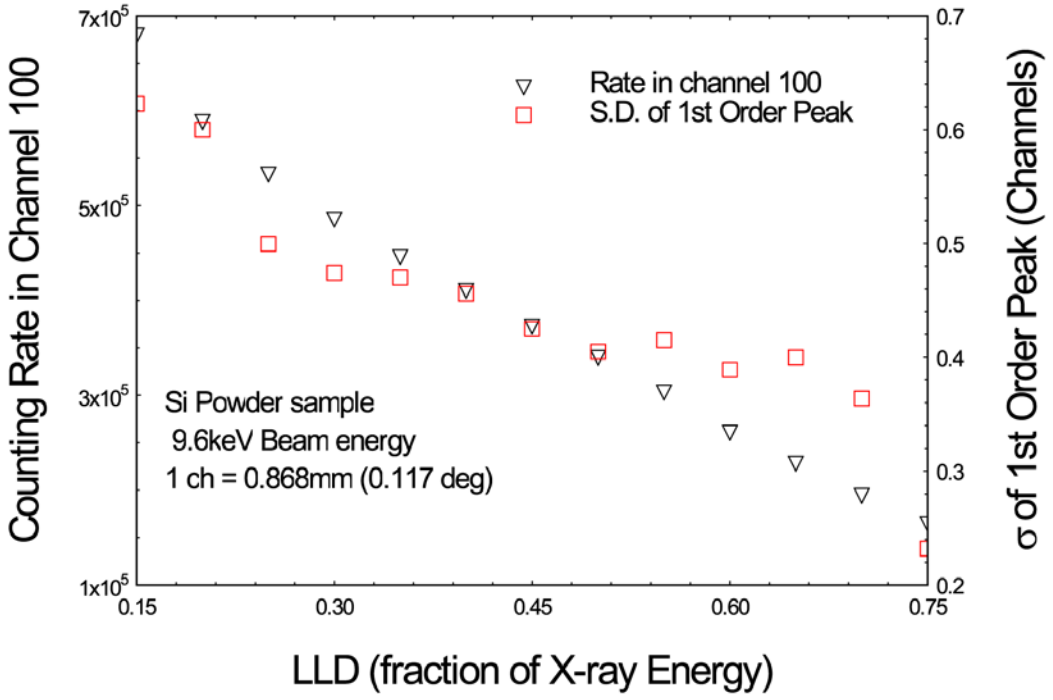

Figure 5: The variation of counting rate and spatial resolution as a function of LLD

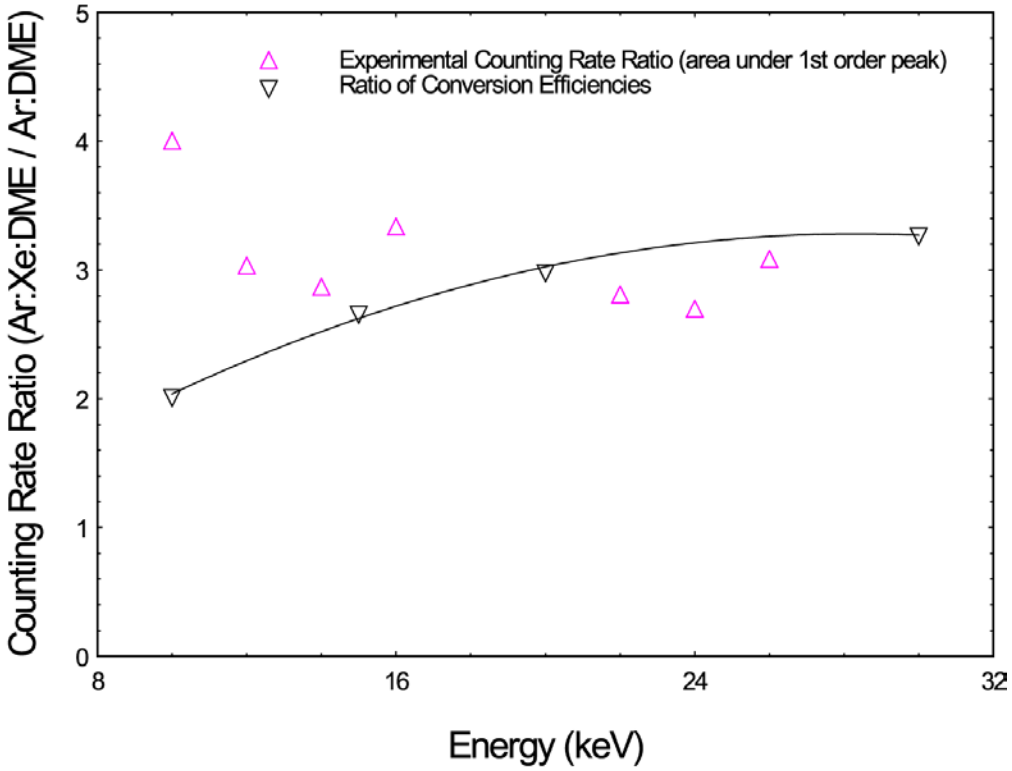

Figure 6: Ratio of experimentally observed counting ratios
in Ar:DME and Ar:Xe:DME mixtures

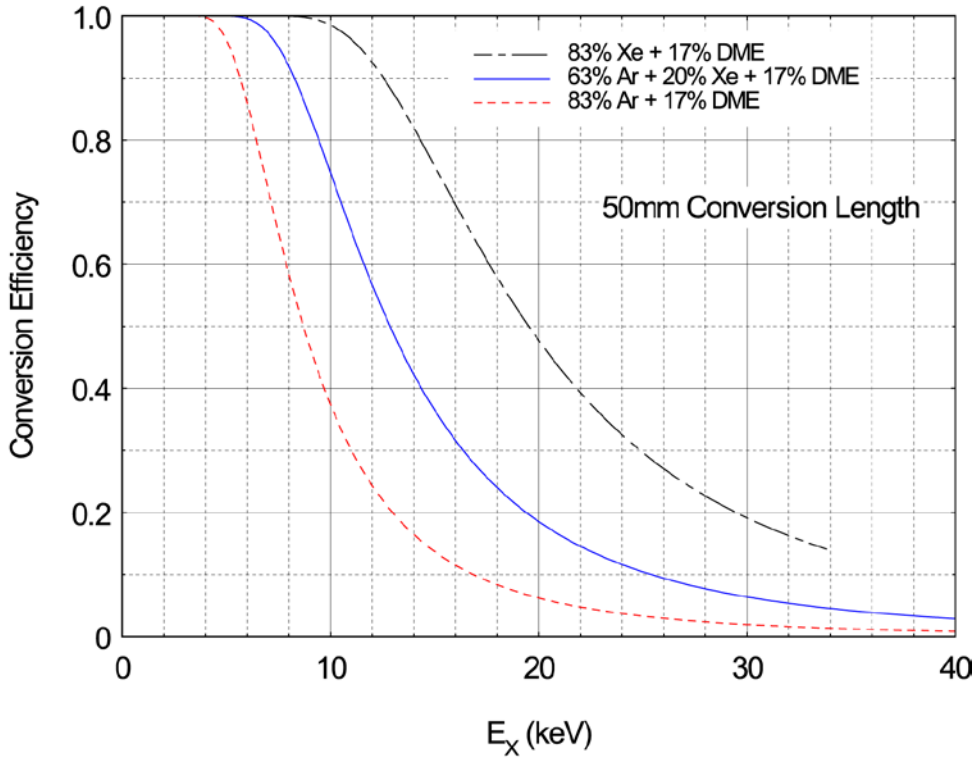

Figure 7: Theoretical conversion efficiencies of the various gas mixtures.

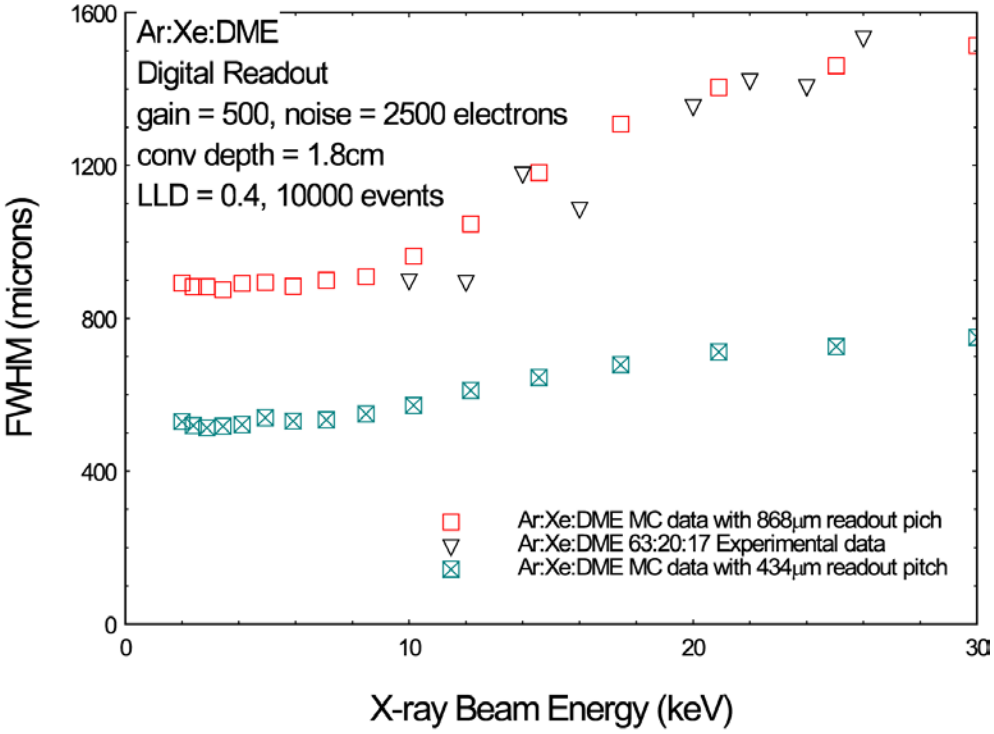

Figure 8: Simulation data showing the improvement in the position resolution at half the current strip pitch

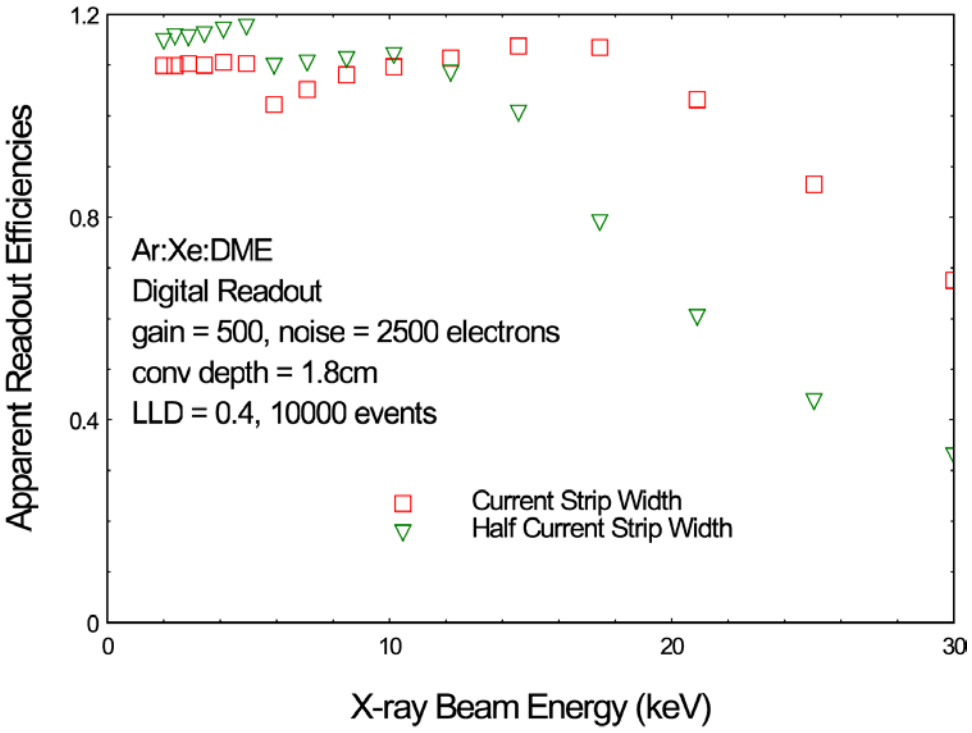

Figure 9: Simulation data showing the predicted variation of the apparent readout efficiency for the two strip pitches